THE JOURNAL OF PHYSICAL CHEMISTRY C

Article

pubs.acs.org/JPCC

Infrared Spectroscopy Investigation of the Acid Sites in the Metal–Organic Framework Aluminum Trimesate MIL-100(Al)

Christophe Volkringer,[†,§] Hervé Leclerc,[‡] Jean-Claude Lavalley,[‡] Thierry Loiseau,[†,§] Gérard Férey,[†] Marco Daturi,[‡] and Alexandre Vimont*[,‡]

[†]Institut Lavoisier, UMR CNRS 8180, Université Versailles-Saint Quentin en Yvelines, 78035 Versailles, France

[‡]Laboratoire Catalyse et Spectrochimie, ENSICAEN, Université de Caen Basse Normandie, CNRS, 6 Bd du Maréchal Juin, 14050 Caen, France

Supporting Information

ABSTRACT: Infrared spectra of MIL-100(Al) have been recorded after evacuation from room temperature up to 623 K. In addition to adsorbed water molecules characterized by specific $(\nu+\delta)H_2O$ combination bands at about 5300 cm^{-1}, spectra analysis shows the presence of impurities like carboxylic acid and nitrates resulting from the synthesis step, explaining the low amount of Al–OH groups detected. The Lewis acidity has been characterized by CO [ν(CO) at 2183 cm^{-1}], pyridine [ν8a band estimated at 1618 cm^{-1}], and CD_3CN [ν(CN) at 2326 cm^{-1}] adsorption on the activated sample. The acidity is strong as revealed by the ν(CN) wavenumber. Interestingly, CO gives rise to an interaction weaker than that expected from pyridine and CD_3CN results. Quantitative results relative to the number of $Al^{3+}{}_{5c}$ sites are in full agreement with those reported elsewhere from ^{27}Al NMR experiments. The Brønsted acidity mainly results from the presence of coordinated water species in the nonfully dehydrated sample and not from the structural Al–OH groups.

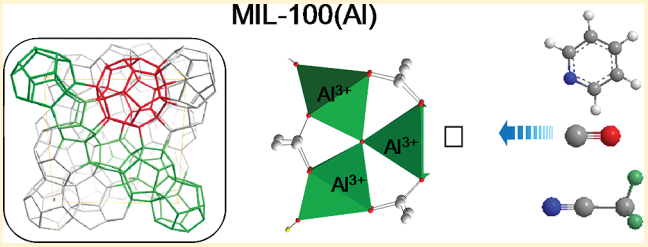

INTRODUCTION

Since the past decade, there has been a growing interest in the synthesis and structural characterization of hybrid organic–inorganic crystalline porous materials, commonly referred to as metal–organic frameworks (MOF) or coordination polymers. Beside the fascinating arrangement and complexity of their networks topologies, some of them exhibit extra large pore systems, which may find applications in many fields (molecule storage or separation, catalysis, drug delivery, etc.).[1−4] In this class of solids, aluminum-based MOF-type compounds have been less investigated compared to the other metallic elements (mainly transition metals with incomplete 3d orbitals) from the periodic table, despite significant industrial interests (low cost, low density, etc.). With the use of multidentate carboxylate linkers, several structural types have already been identified. A large number of these compounds are defined from 1D infinite chains of AlO_6 octahedra, generating lozenge-shape channels (MIL-53[5] and derived types[6−17] with functionalized ligands or increasing number of benzene rings), while a few members are built up from discrete motifs of aluminum centers with variable nuclearities.[18−25] Among the different building blocks, the μ_3-oxo-centered trinuclear unit $(M_3(\mu_3\text{-}O)(O_2C\text{-}R)_6$, M = trivalent or bivalent metal) has attracted a special attention since extra large pore materials and/or highly flexible frameworks are based on the 3D connection of this trimer.[26,27] With aluminum, this trinuclear entity was first isolated in molecular assemblies[28,29] and then encountered in different extended 3D networks such as MIL-96,[30] MIL-100,[20] MIL-101,[21] or more recently in the MOF-235[23,24] type (or MIL-88B).

The use of IR spectroscopy appears as a tool of choice to study these materials presenting a huge surface area.[31−33] Moreover it allows monitoring gas sorption (CO, H_2, NO, C_2H_4)[34,35] or intermediate species during catalytic reactions.[36] Indeed, the change of vibrational frequencies can give substantial information concerning the strength of the interactions occurring at the material surface and the nature of the adsorbed molecules.[36,37] During the last decades, IR spectroscopy was intensively employed to characterize the type and the strength of the acid sites using probes like CO,[38] pyridine,[39] and acetonitrile.[40] In particular in the case of aluminum-based inorganic solids such as oxides,[41] supported metals,[42] and zeolites.[37,43] In general, a good agreement in the acidity order is observed whatever the probe used,[40,41] and the strength of different sites according to their unsaturation or the presence of coordinative defects can be distinguished. For instance, it has been reported on alumina that the Lewis acid strength of $Al^{3+}{}_{3c}$ is much higher than that of $Al^{3+}{}_{5c}$.[44,45] However in specific cases like silica-boria, a discrepancy between the results obtained from soft bases like CO and strong one like pyridine has been reported and related to the conformational change of the adsorption site due to the

Received: November 7, 2011
Revised: February 3, 2012
Published: February 3, 2012

   dx.doi.org/10.1021/jp210671t | J. Phys. Chem. C 2012, 116, 5710–5719

adsorption.[43,46] From a more general point of view, the strength of an acid and a conjugate base are interdependent and regulated by their relative electronegativity and hardness.[47,48] If the surface structure presents a sufficient flexibility, a strong basic probe molecule (such as pyridine) can polarize a cation much more than a weaker molecule (such as CO), thus revealing a higher acidity.[49]

In this contribution, we report the investigation of the thermal behavior and the interaction of the aluminum centers with different probe molecules (CO, pyridine, acetonitrile, etc.), for the aluminum version of the trimesate MIL-100[20] $Al_3O(btc)_2(OH)(H_2O)_2{\cdot}X$ (btc = benzenetricarboxylate; X = encapsulated species, i.e., H_2O, etc.) by using infrared spectroscopy. The MIL-100 topology was previously characterized with trivalent chromium[50] or iron[51] and is related to the cubic MTN zeolite structural type.[52] It contains trinuclear building blocks linked to each other through the trimesate ligands in order to build a supertetrahedral (ST) unit (each corner corresponds to an inorganic trimer whereas the faces are covered by the aromatic ring of the organic linker). The supertetrahedrons, reminiscent of the silicate SiO_4 primary building unit found in zeolites family, are then corner-shared in such a way to construct a 3D framework based on the stacking of two types of cavities. One is delimited by 12 pentagonal windows with 5.2 Å size (dodecahedral cage); the second is delimited by 12 pentagonal windows and 4 hexagonal windows with 8.8 Å size (hexakaidodecahedral cage).[53] In this compound, aluminum is octahedrally coordinated with four carboxyl oxygen atoms (from carboxylate arms of trimesate), one μ_3-oxo group and one aquo or hydroxo group in terminal position. Upon heating, the terminal aquo species can be removed and lowers the coordination state of the metal center. A previous NMR study[54] clearly showed the coordination lowering with the occurrence of 5-fold coordinated aluminum when removing the terminal water molecule. The aim of this work is the infrared investigation of these coordinatively unsaturated sites (CUS) for aluminum as a function of temperature and the analysis of the influence of different probe molecules such as carbon monoxide, pyridine, acetonitrile. An estimation of the acid strength of 5-fold CUS Al^{3+} can be therefore obtained; considering that the presence of a large amount of such sites on the surface of divided materials is scarce, in the present case their high concentration will offer the possibility to work with a greater IR signal.

EXPERIMENTAL SECTION

Synthesis. A sample of MIL-100(Al) was prepared by following the synthetic hydrothermal procedure previously described in the literature.[20,54] After hydrothermal treatment, the resulting yellowish powder was washed with deionized water and dried at room temperature in air atmosphere. 500 mg of as-synthesized slurry was then dispersed in 40 mL of *N*,*N*-dimethylformamide (DMF) and placed in an Teflon-lined Parr type autoclave for 5 h at 423 K. After heating and filtration, the white powder was calcined at 573 K for 5 h in order to evacuate encapsulated DMF species (activated MIL-100(Al)).

Infrared Spectroscopy. Samples of MIL-100(Al) were pressed (~10^6 Torr) into self-supported disks (2 cm^2 area, 7–10 $mg{\cdot}cm^{-2}$). The pellets were placed in a quartz cell equipped with KBr windows. A movable quartz sample holder allows adjusting the pellet in the infrared beam for spectra acquisition and to displace it into a furnace at the top of the cell for thermal treatments. The cell was connected to a vacuum line for evacuation (residual pressure = 10^{-3}–10^{-4} Pa), calcination steps, and for the introduction of gases and vapors into the infrared cell. Transmission IR spectra were recorded in the 500–5600 cm^{-1} range, with a 4 cm^{-1} resolution, on a Nicolet Nexus spectrometer equipped with an extended KBr beam splitting device and a mercury cadmium telluride (MCT) cryodetector.

The acidity of the above material was studied by IR spectroscopy, using adsorbed pyridine, CO, and acetonitrile as spectroscopic probe molecules. CD_3CN has been used instead of CH_3CN in order to directly assess to the ν(CN) frequency unaffected by Fermi resonance interaction. CD_3CN, pyridine (Aldrich, 99+% grade), and CO (99.5%, provided by Air Liquide) were dried on molecular sieves prior to their use. The isotopic purity of CD_3CN was 99.95%. In CO adsorption experiment, the temperature of the pellet was decreased to about 100 K by cooling the sample holder with liquid N_2 after quenching the sample from the thermal treatment temperature. The addition of accurately known increments of CO probe molecules in the cell (a typical increment corresponds to 100 μmoles of CO per gram of material) was possible via a calibrated volume (1.75 cm^3) connected to a pressure gauge for the control of the probe pressure (0–10^4 Pa range). The CO pressure inside the IR cell was controlled by another pressure gauge (0–10^3 Pa range).

RESULTS

Thermal Behavior. The activated MIL-100(Al) compound was characterized by in situ IR spectroscopy at room temperature and after outgassing at different temperatures (RT, 403, 473, 523, 573, and 623 K).

Between 1700 and 1250 cm^{-1}, the IR spectrum of the self-supported pellet displays very intense bands due to carboxylate groups and phenyl ring deformations. This is the reason why the spectra are only presented above 1650 cm^{-1} region and in the region between 1200 and 950 cm^{-1}, where a transmission window is present. The spectrum of MIL-100(Al) evacuated at 403 K shows two shoulders at 1740 and 1760 cm^{-1} (Figure 1b). The lower wavenumber (1740 cm^{-1}) band disappears around 523 K, whereas the intensity of the second one (1760 cm^{-1}) decreases at higher temperature but is still visible at 623 K even with a very weak intensity (Figure 1f). Both bands characterize the ν(C═O) mode of carboxyl groups of the trimesic acid; this assignment is in good agreement with the chemical elemental analysis which revealed an excess of carbon,[54] which could be assigned to residual extra framework trimesic acid molecules.

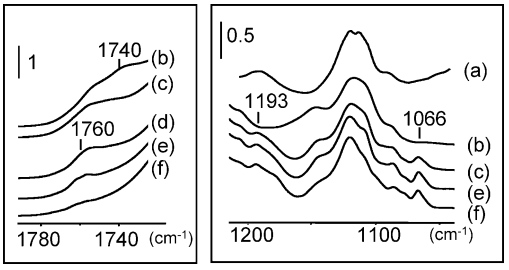

Figure 1. Infrared spectra of MIL-100(Al) in the 1800–1700 cm^{-1} and 1200–1000 cm^{-1} ranges after evacuation at (a) room temperature, (b) 403 K, (c) 473 K, (d) 523 K, (e) 573 K, and (f) 623 K.

dx.doi.org/10.1021/jp210671t | J. Phys. Chem. C 2012, 116, 5710–5719

At lower wavenumbers, in addition to the isolated band (1120 cm^{-1}) due to ring deformation modes of the trimesate linker,[55] weak bands are detected at 1066, 1175, and 1193 cm^{-1} in the spectrum of the sample heated at 473 K; they are still present after heating up to 623 K (Figure 1f). These bands are sensitive to the presence of water since they are not observed for the room temperature activated sample (Figure 1a) or after heating at 623 K followed by rehydration (Figure S1 of Supporting Information). These bands are specific to MIL-100(Al) since none of them is observed in the IR spectrum of the activated parent MIL-100(Cr) (Figure S1 of Supporting Information). According to the chemical elemental analysis,[54] these bands could be attributed to the presence of nitrogen-derivated species (i.e., nitrate, etc.). It is worth noting that, contrary to MIL-100(Cr), the synthesis of MIL-100(Al)[20] involves nitric acid in the synthesis media ($Al(NO_3)_3{\cdot}9H_2O$ is used as precursor and HNO_3 is added to the mixture). The other possible source of nitrogen could come from decomposition products of DMF (used as solvent during the activation process) but not the DMF itself according to the absence of $\nu(CH_3)$ bands characteristic of the methyl groups at about 2930 cm^{-1}. Moreover, the comparison of the spectra of MIL-100(Al) samples (nonactivated and activated one) with different nitrogen contents shows that the intensities of the bands at 1066 and 1193 cm^{-1} increase with nitrogen amount (Figure S2 of Supporting Information). The corresponding observed wavenumbers are expected to be one of the ν_3 doubly degenerated modes (1193 cm^{-1}, the second for bridged nitrates over Al sites being expected near 1600 cm^{-1}, therefore hidden by the carboxylate bands) and ν_1 mode (1066 cm^{-1}) of NO_3^- species.[56] Therefore, the presence of thermally stable extra framework nitrate species should be considered, even if on oxide surfaces they are known to be at the limit of their stability at such a temperature.[57]

Terminal Hydroxy Groups and Water. To differentiate bands of water from those of hydroxy groups expected from the framework chemical formula $Al_3O(btc)_2(OH)(H_2O)_2$, different frequency ranges have been studied. In the case of MIL-100(Cr), the Cr−OH groups lead to a ν(OH) band at 3585 cm^{-1}, identified with respect to water features thanks to the absence of a combination band in the 5000−5400 cm^{-1} range.[33] In fact, vibrations specific to water are those involving the $\delta(H_2O)$ mode, either the fundamental mode near 1630 cm^{-1} (in the case of MOFs not directly accessible due to the strong carboxylate bands) or its combination $\nu+\delta(H_2O)$ characterized by bands in the 5000−5300 cm^{-1} range. The study of the latter allows differentiating the various oligomeric water species: for example, terminal water can be bonded to aluminum centers only (complex 1:1); bonded terminal water can interact through hydrogen bond to one (complex 1:2 or second hydration sphere) or several extra framework water molecules ("multimer") (scheme 1). The latter cases (complex 1:2 or "multimer") are expected to generate bands around 5320 and 5250 cm^{-1}, whereas the monocoordinated water species (complex 1:1 or first hydration sphere) on coordinatively unsaturated sites of aluminum (CUS) should be characterized by bands between 5265 and 5274 cm^{-1}.[33,32]

Scheme 1. Interaction of Water Molecules with Al^{3+} CUS in MIL-100(Al)

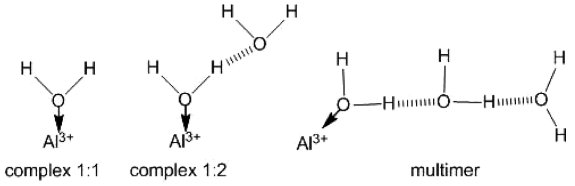

In the present case, the entire $\nu+\delta(H_2O)$ massif (Figure 2) decreases in intensity by heating the sample under vacuum

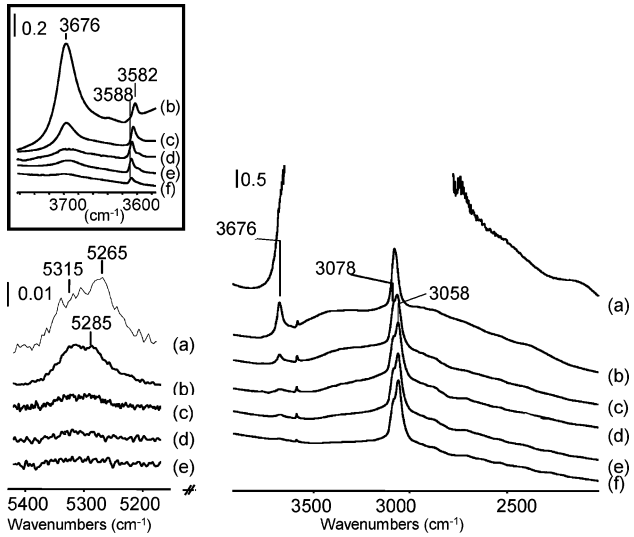

Figure 2. Infrared spectra of MIL-100(Al): (a) under room atmosphere and then under vacuum for two hours at (b) 403 K, (c) 473 K, (d) 523 K, (e) 573 K, and (f) 623 K; details for the ν(OH) range are provided in the insert.

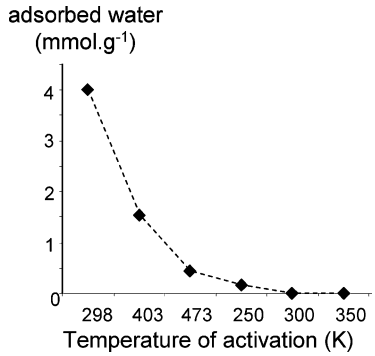

Figure 3. Water content vs the temperature of activation of MIL-100(Al).

from room temperature up to 473 K, and then it almost disappears at 623 K. By consideration of the molar absorption coefficient reported in the literature for this massif (0.22 cm.$\mu$$mol^{-1}$),[58] it is possible to quantify the amount of adsorbed water as a function of the heating temperature (Figure 3). It appears that the majority of water desorbs from room temperature to 403 K under vacuum, in agreement with the NMR results.[54] Note that the NMR water signal is still observable at 473 K, in agreement with the persistence of the weak $\nu+\delta(H_2O)$ IR band at 5300 cm^{-1} after the vacuum treatment at a similar temperature (Figure 2c).

On activated MIL-100(Al) under vacuum at room temperature (Figure 2a.), we observe a complex and ill-defined massif, among which two broad bands at 5315 and 5265 cm^{-1} emerge; they are assigned to water in hydrogen bond interactions with extra framework water (complex 1:2 or multimer, as indicated

dx.doi.org/10.1021/jp210671t | J. Phys. Chem. C 2012, 116, 5710−5719

in Scheme 1). Degassing at 403 K (Figure 2b) eliminates the low-frequency component near 5265 cm^{-1} resulting in the emergence of a band at around 5285 cm^{-1}, badly resolved in the spectrum after evacuation at room temperature. This change is due to the departure of hydrogen bonded water species (mainly multimer) between room temperature and 403 K, while the coordinated species are less affected. Nevertheless, the persistence of a weak shoulder above 5300 cm^{-1} in the IR spectrum of the solid degassed at 473 and 523 K (parts c and d of Figure 2) indicates the occurrence of some multimeric water molecules in addition to isolated coordinated species 1:1 at such temperatures. The study of the combination bands makes easier the assignments in the ν(OH) range, where the presence of a large amount of water after evacuation at room temperature gives rise to the occurrence of strong bands at 3676 (sharp) and 3000 cm^{-1} (broad) (Figure 2). This couple of vibrations is attributed to strongly hydrogen-bonded water molecules (complex 1:2 and "multimer"). Similar observations were made for the parent MIL-100(Cr)[33] and MIL-100(Fe).[31] In the same frequency range, a sharp band at 3078 cm^{-1} is assigned to framework ν(CH) vibrations (see below). The wavenumber of the band at 3676 cm^{-1} remains invariant whatever the heating temperature, but the emerging of an additional band at 3582 cm^{-1} together with a shoulder at 3588 cm^{-1} is observed after evacuation at 403 K. At 473 K this shoulder becomes predominant, while the 3582 cm^{-1} component is disappearing. The spectrum after heating at 623 K only shows ν(OH) bands with a very low intensity. However, the 3588 cm^{-1} band is still well detected (Figure 2f), and its intensity cannot be related to another combination band, suggesting that it is the signature of terminal Al−OH groups. In the case of MIL-100(Cr) the same band was observed and attributed to (Cr)−OH groups.[33] The intensity of this band for MIL-100(Cr) and MIL-100(Al) is compared in Figure S3 of Supporting Information. The spectra of MIL-100 (Cr) and MIL-100 (Al) evacuated at 573 K are normalized to the same mass (10 mg); the spectra present a band at 1120 cm^{-1} of the same intensity, confirming the normalization validation. The intensity of the ν(OH) band of MIL-100(Al) is at least 3−4 times weaker than that of MIL-100 (Cr). We may conclude that MIL-100(Al) should contain less M−OH groups than MIL-100(Cr).

Above 473 K, the couple of bands located at 3676 and 3582 cm^{-1} (parts c and d of Figure 2) is still visible and assigned to complex 1:1 (terminal water). This indicates a strong interaction of the water molecules for MIL-100(Al). In the case of MIL-100(Cr) or MIL-100(Fe), the coordinated water molecules (complex 1:1) were characterized by two bands ν_{as} and ν_s at about 3700−3680 and 3610−3590 cm^{-1}, respectively, and disappeared by evacuation at 473 K (Cr) or 373 K (Fe).

Study of Benzene CH Groups. For the sample evacuated at room temperature, ν(CH) vibrations of aromatic rings only give rise to an intense band located at 3078 cm^{-1}. It was reported at 3088 cm^{-1} for MIL-100(Cr) and at 3090 cm^{-1} for MIL-100(Fe). Interestingly, upon heating, the intensity of the band at 3078 cm^{-1} decreases, whereas a new band at 3058 cm^{-1} appears from 473 K (Figure 4A). The isosbestic point at 3068 cm^{-1} shows that the two phenomena are correlated; moreover they are reversible, since the addition of water on the activated compound gradually eliminates the low frequency band and completely restores that at 3078 cm^{-1} (Figure 4B). This phenomenon is very clear in the case of MIL-100(Al) but is hardly noticeable in the case of MIL-100(Cr). The conversion

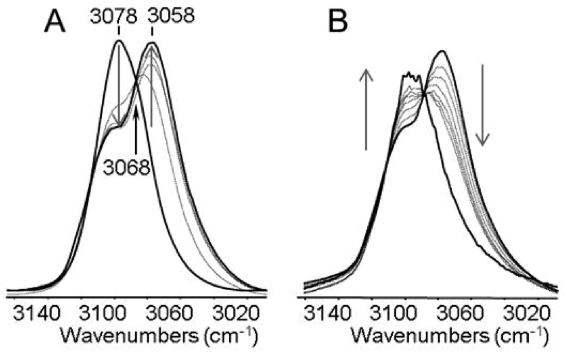

Figure 4. ν(CH) band of MIL-100 (Al) (A) during activation from room temperature to 623 K and (B) during progressive additions of water at room temperature on the sample activated at 623 K.

is not complete since about 10% of the intensity of the 3078 cm^{-1} band persists after complete water elimination, suggesting that the 3078 cm^{-1} band is due to two different trimesate configurations as discussed below.

Acid Properties. *Adsorption of CO at 100 K on MIL-100 (Al) activated at 623 K.* The first addition of CO at 100 K (56 μmol g^{-1}) gives rise to a ν(CO) band at 2210 cm^{-1} (Figure 5a); its intensity does not increase further by adding supplementary doses of CO, which leads to the appearance of an additional band at 2195 cm^{-1}; on the contrary the intensity of the latter increases while its wavenumber shifts to 2183 cm^{-1} (parts b−d of Figure 5). After saturation, there is a weak band at 2154 cm^{-1}, characterizing the formation of H-

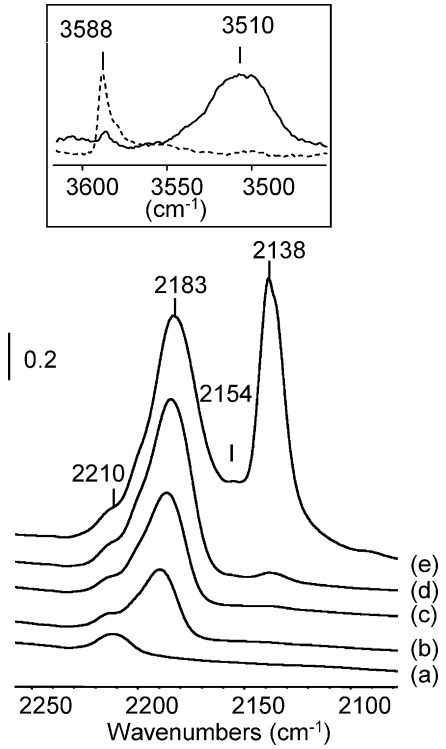

Figure 5. Infrared spectra recorded at 100 K of MIL-100(Al) after activation at 573 K and introduction of increasing doses of CO: from 56 μmol g^{-1} (a) to 900 μmol g^{-1} (d) and then introduction of an equilibrium pressure (1333 Pa) (spectrum e). Insert: Spectrum of MIL-100(Al) activated at 573 K before (dotted line) and after (full line) introduction of an equilibrium pressure of CO at 100 K.

dx.doi.org/10.1021/jp210671t | J. Phys. Chem. C 2012, 116, 5710−5719

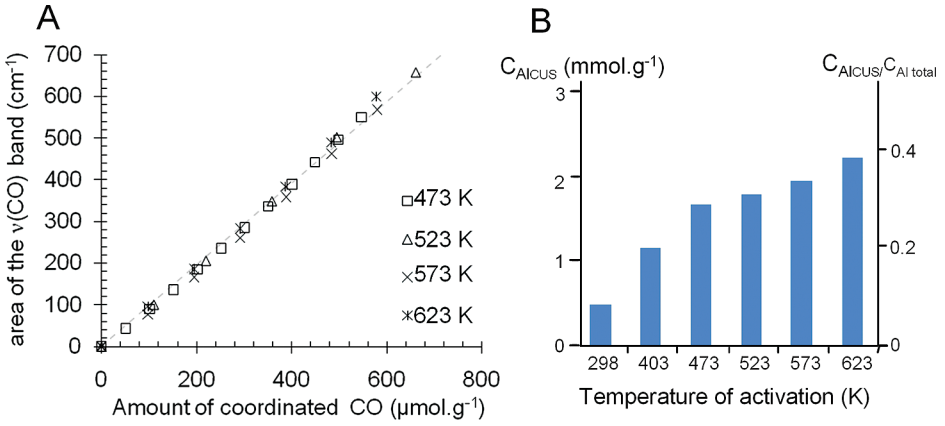

Figure 6. (A) Integrated area of ν(CO) bands of coordinated species (2180−2220 cm^{-1} range) vs the concentration of CO introduced at 100 K into the IR cell vs the temperature of activation. (B) Variation of the concentration of Al^{3+} CUS detected by CO on MIL-100(Al) vs the temperature of activation.

bonded species, and two bands at 2138 and 2135 cm^{-1} due to physisorbed species (Figure 5e). In the region of hydroxyl vibrations, only two bands at 3676 cm^{-1} (broad) and 3588 cm^{-1} (weak) persist after heating at 623 K. Both are perturbed under an equilibrium CO pressure (666 Pa) shifting toward lower wavenumbers: in particular, the 3588 cm^{-1} band gives rise to a broader one at 3510 cm^{-1} (Figure 5 insert). Regarding the region of ν(CH) vibrations, the two bands at 3058 and 3078 cm^{-1} do not seem affected whatever the amount of CO adsorbed, although a slight decrease in intensity is noted. As concerned the couple of bands at 1066 and 1193 cm^{-1}, CO adsorption upward shifts them of about 8−9 cm^{-1}. This confirms that these two bands are associated to the same species.

By analogy with oxides, the weak ν(CO) band at 2210 cm^{-1} would be attributed to particular Al defects with a high Lewis acidity, while the main ν(CO) band (2195−2184 cm^{-1}) corresponds to CO adsorption on a large amount of CUS Al^{3+} cations resulting from water elimination.[59] A previous NMR study[54] clearly described the occurrence of the pentacoordinated aluminum sites related to the unsaturated site (CUS) mentioned previously.

Quantification of the Number of Al^{3+} CUS. To obtain quantitative results, CO has been introduced by calibrate aliquots at 100 K, to measure the ν(CO) molar absorption coefficient, considering that under such conditions at low coverage the whole CO introduced is adsorbed on the sample surface. As shown in Figure 6A, introduction of CO on MIL-100(Al) activated at 623 K provokes the linear increase in the intensity of the 2195−2184 cm^{-1} band, characterizing the formation of CO species coordinated to CUS Al^{3+}. Its molar absorption coefficient calculated from the slope of the line is equal to 2.0 μmol^{-1} cm and does not depend on the activation temperature of the sample, since the data relative to the samples activated from 473 to 673 K fit on the same straight line. The value of the adsorption coefficient so obtained is similar to that reported for ν(CO) bands of CO species coordinated on Cr^{3+} CUS in MIL-100(Cr).[33]

Knowing the molar absorption coefficient of the main ν(CO) band, it is possible to determine the number of the corresponding CUS Al^{3+} depending on the sample activation temperature, as reported in Figure 6B. The increase in the number of Al^{3+} CUS up to 473 K is related to the departure of coordinated water. Above 523 K, the intensity increase is still continuous but less intense, and it can be associated to the departure of extra framework organic species characterized by the 1760−1740 cm^{-1} bands. The amount of coordinated CO on the CUS reaches the 2.2 $mmol.g^{-1}$ for the sample activated at 623 K.

Adsorption of Pyridine. Pyridine was introduced on the MIL-100(Al) evacuated at 573 K. The sample pellet was then heated under vacuum at 373 K to evacuate physisorbed pyridine. The IR spectrum displays three bands at 1018, 1051, and 1074 cm^{-1} assigned to the ν_1, ν_{12}, and ν_{18a} modes of pyridine coordinated to Al^{3+} CUS, respectively (Figure 7). It

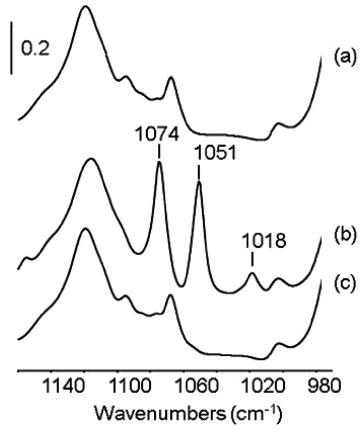

Figure 7. (a) Infrared spectra of MIL-100 (Al) activated at 573 K under vacuum; (b) after introduction of pyridine (133 Pa at equilibrium pressure) at 373 K followed by evacuation at the same temperature; (c) outgassing at 553 K.

has been previously reported that a linear relationship exists between the ν_1 and ν_{8a} mode wavenumbers from observations relative to pyridine coordination on several oxides.[31] From this relation, the ν_{8a} band position (not directly observable in our case) can be deduced from the ν_1 band (1018 cm^{-1}) observed for coordinated pyridine on MIL-100(Al): it should be expected close to 1616−1618 cm^{-1}. On alumina, three bands are detected upon pyridine adsorption, one at ∼1625 cm^{-1} and another at a similar position (1618 cm^{-1}) for coordinated pyridine, the third been at 1595−1600 cm^{-1}. The two first have been related to CUS Al^{3+} in tetrahedral coordination, while the latter to octahedral species.[60,61] Regarding the region of the

dx.doi.org/10.1021/jp210671t | J. Phys. Chem. C 2012, 116, 5710−5719

framework ν(CH) vibrations, the band at 3058 cm^{-1} is clearly affected by the presence of coordinated pyridine: its intensity decreases, whereas that at 3078 cm^{-1} increases, and the 3058 cm^{-1} is then restored after pyridine evacuation at 553 K.

The amount of pyridine coordinated to Al^{3+} CUS can be estimated using the molar absorption coefficient of the ν_{12} and ν_{18a} bands determined by adsorption of calibrate doses of pyridine. In MIL-100(Cr), the coefficients were 0.5 and 0.6 cm μmol^{-1}, respectively. By use of these values, such amount is equal to about 1.9 (±0.200) mmol g^{-1} for MIL-100(Al) activated at 573 K, which is close to the amount of coordinated CO, as reported in Figure 6. This shows that the CUS Al^{3+} have a similar accessibility to these two probe molecules.

Adsorption of CD_3CN. The adsorption of acetonitrile on MIL-100 (Al) activated at 553 K (Figure 8a) gives rise to two

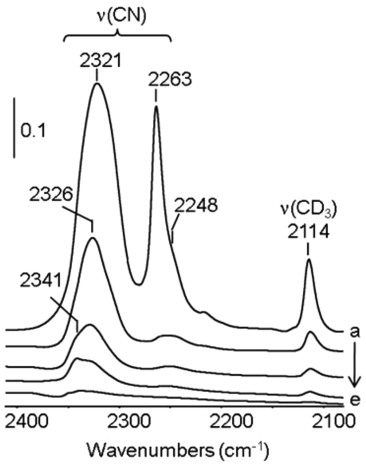

Figure 8. Infrared spectra of MIL-100 (Al) activated at 553 K (a) after introduction of acetonitrile into the cell (9330 Pa), followed by evacuation at (b) room temperature, (c) 323 K, (d) 373 K, (e) 423 K.

main ν(CN) bands denoting the presence of physisorbed (ν(CN) = 2263 cm^{-1}) and coordinated species on Al^{3+} CUS (ν(CN) = 2321 cm^{-1}).[41] A band at 2114 cm^{-1} is attributed to the $\nu(CD_3)$ vibration of adsorbed deuterated acetonitrile. After evacuation at room temperature, the ν(CN) band intensity of physisorbed species strongly decreases (Figure 8b), while the band characterizing the acetonitrile coordinating Al sites slightly decreases in intensity and shifts to 2326 cm^{-1}. Evacuation at higher temperature (323, 373, and 423 K) indicates a weak ν(CN) band at 2341 cm^{-1} (shoulder), which is assigned to Al defects with a higher Lewis acidity. In the ν(CH) range, the intensity of the framework band at 3058 cm^{-1} strongly decreases in presence of acetonitrile, together with the growth of the band at 3078 cm^{-1}. After removal of acetonitrile by degassing, the spectrum recovers its original shape.

Evolution of the Brønsted Acidity with the Temperature of Activation. CO adsorption at 100 K has been repeated on MIL-100(Al) activated at different temperatures. When the sample is evacuated at room temperature, a strong band is visible at 2154 cm^{-1} (Figure 9a) in addition to that corresponding to physisorbed species (2138 cm^{-1}). The 2154 cm^{-1} frequency could correspond to the presence of weak Lewis acid sites, as reported on α-alumina, sample presenting $Al^{3+}{}_{5c}$ species.[45] However, its intensity is strong when the sample is activated at low temperature, i.e., when a large amount of water is adsorbed on the surface (strong band at 3676 cm^{-1}). When the sample is activated at 573 K, the 2154

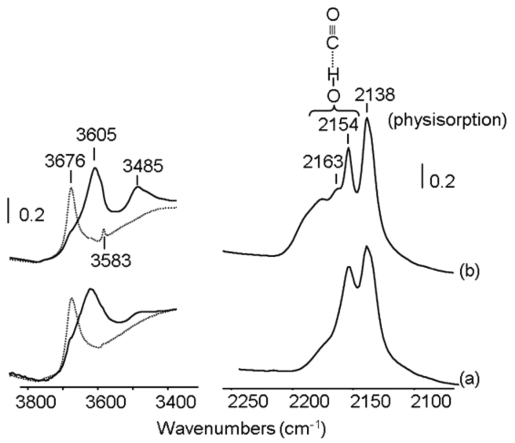

Figure 9. Infrared spectra recorded at 100 K of MIL-100(Al) activated at (a) room temperature and (b) 403 K, before (dotted line) and after (full line) introduction of an equilibrium pressure of CO (133 Pa).

cm^{-1} band intensity is very weak, showing that it does not characterize Lewis acidity; we therefore assign it to CO interacting through hydrogen bond to hydroxyl groups (Brønsted acidity). Such an assignment is confirmed by the good correlation between the ν(CO) frequency and the perturbation of hydroxyl groups as shown hereafter. On the fully hydrated sample, the 2154 cm^{-1} band characterizes the acidity of hydroxyl groups of adsorbed water species. The ν(OH) band at 3676 cm^{-1} shifts to 3605 cm^{-1} and characterizes the Brønsted acidity of water multimeric species, as in the case of MIL-100(Cr).[32] CO adsorption on the sample activated at 403 K shows the appearance of a few amount of stronger acid sites (weak ν(CO) at 2163 cm^{-1}), which is related to the presence of a perturbed ν(OH) band at 3485 cm^{-1} (Figure 9b). By analogy with results reported for MIL-100(Cr),[33] such a band corresponds to CO interacting with free OH groups of water (complex 1:1, see Scheme 1). This shows that water evacuation at 403 K transforms weak acidic complexes 1:2 into more acidic complexes 1:1. When heating at higher temperature (>523 K), water is completely evolved and the presence of the ν(CO) band at 2154 cm^{-1} is assigned to CO adsorption on framework terminal Al−OH groups (Figure 5), the wavenumber of the corresponding ν(OH) band shifting from 3588 to 3502 cm^{-1}.

DISCUSSION

CUS $Al^{3+}{}_{5c}$ Concentration and Extra Framework Chemical Impurities. Previous thermal behavior of MIL-100(Al) was analyzed by solid-state NMR and series ^{27}Al spectra showed an evolution of the coordination state for aluminum centers. They are 6-fold coordinated at room temperature, but some of them exhibited 5-fold coordination environments (resonance signal at 30−40 ppm) due to the removal of terminal water after heating under vacuum at high temperature. This dehydration process involves the formation of CUS, which can be highlighted by infrared spectroscopy upon adsorption of probes molecules like CO, acetonitrile, or pyridine. ^{27}Al NMR analysis determined that one-third of aluminum is pentacoordinated in the dehydrated form. A good quantitative agreement is also observed by IR. The present study shows that about 2.2 mmol g^{-1} of CO or 1.9 mmol g^{-1} of pyridine are coordinated on such defective sites. Considering the mass of the dried sample deduced from TGA analysis

dx.doi.org/10.1021/jp210671t | J. Phys. Chem. C 2012, 116, 5710−5719

measurement, such values show that 35−40% of the total amount of aluminum ions presents a Lewis acidity, i.e., a coordinative unsaturation (Figure 6b). This number is lower than expected if all the aluminum moieties would have been affected by water removal. In fact, by consideration of the chemical formula for MIL-100(Al): $Al_3O(btc)_2(H_2O)_2(OH)$), 66% of the Al species could potentially generate coordinatively unsaturated sites. This differs from the result observed for MIL-100(Cr) or MIL-100(Fe), where the expected number of CUS ($^2/_3$) was effectively measured by CO adsorption experiments.[31,33]

By consideration of the chemical elemental analysis of activated MIL-100(Al), the excess of carbon (23.75% instead of 20.75%), and the presence of nitrogen (0.23%) would involve the existence of extra framework molecules such as unreacted trimesic acid or nitrogen containing species ($[Al_3O(btc)_2(H_2O)_2(OH)]\cdot(H_2O)_{22-25}(H_3btc)_{0.3}(HNO_3)_{0.2}$).[54] The presence of nitrate-like species could be related to the bands at 1193 and 1066 cm^{-1}. Moreover, the ^1H NMR experiment has shown the presence of extra framework trimesic acid species (resonance peak at 8.0 ppm), which could interact to aluminum cations through a monodentate bridging mode. Infrared experiments also agree with the presence of trimesic acid through the observation of carboxylic bands (1740−1760 cm^{-1}), which tend to decrease upon heating. Both H_3btc or HNO_3 can act as poisoning agents for the Al CUS. Some of them, in deprotonated form, could substitute some terminal OH groups and play the role of counteranion, which partly explains the weaker amount of detected hydroxyl groups. A possibility is the formation of grafted trimesate species involving some terminal hydroxyl groups, explaining the weak intensity of the ν(OH) band at 3588 cm^{-1}. The study of the sensitivity of the ν(CH) bands to adsorbates like water reveals that 10% of the intensity of the ν(CH) band of trimesate species at 3078 cm^{-1} is not sensitive to the coordination of probes like water and pyridine. The sensitive behavior would be specific to trimesate groups in the MIL-100(Al) framework, whereas the species unaffected by probe molecule adsorption (10%) would be characteristic of trimesate groups in an extra framework position (impurities), or caused by the inaccessibility of a portion of sites, due to the presence of impurities in the porosity.

Lewis Acidity. From the infrared spectroscopic point of view, the main interest of the MIL-100(Al) sample is the formation of a large content of CUS $Al^{3+}{}_{5c}$ after dehydration (occurrence of 5-fold coordinated aluminum atoms). Only a few numbers of studies have reported the acidity of such aluminum cations. In the present sample aluminum is expected to be in octahedral coordination, therefore pentacoordinated $Al^{3+}{}_{5c}$ cations are expected to be formed from the dehydration. A similar phenomenon is expected to occur on the surface of α-alumina by dehydroxylation, but such a material presents a very low surface area, leading to very weak ν(CO) bands.[45] Octahedral species are present also in the high surface area γ-alumina, but the concomitant presence of tetrahedral entities (together with different defects), makes their identification questionable. Generally, it is accepted that their wavenumber is quite low, close to 2160 cm^{-1},[44,45] and therefore much lower than that observed in the MOFs structure (2194−2185 cm^{-1}). Such a result makes the parallel with those of Bordiga et al. about CO adsorption on CPO-27(Ni) sample, where it was reported that the ν(CO) frequency of coordinated carbonyls on Ni^{2+} decreases in the following order: cations in zeolites > MOFs > nickel oxides.[62] Therefore, we should conclude that the polarizing power of the cations in MOFs is higher than in the corresponding oxides due to the difference in the electronegativity between the organic linker in the hybrid structure and the oxygen in the metal oxide.

In Table 1, we report the strength of the Lewis acid sites obtained from CO, pyridine and CD_3CN adsorbed on MIL-100(Fe), MIL-100(Al), and MIL-100(Cr). Taking into account the charge to radius ratio of the M^{3+} ions, the following order is expected concerning their polarizing power: Al^{3+} > Fe^{3+} > Cr^{3+}.[63]

Table 1. Typical Wavenumbers of Several Coordinated Probe Molecules on MIL-100 Materials

material	CO (ν(CO) cm^{-1})	CD_3CN (ν(CN) cm^{-1})	pyridine (ν_1 cm^{-1})
MIL-100(Al)	2195−2184	2326−2321	1018
MIL-100(Fe)[31]	2192−2173	2304	1014
MIL-100(Cr)[33]	2207, 2200, 2196	2305	1015

Pyridine and acetonitrile adsorptions confirm the higher acid strength for Al^{3+} cations, even if no difference is pointed out between iron and chromium. Let us remark that the ν(CN) wavenumber observed in the present study (2326−2321 cm^{-1}) is consistent with the frequency (2327 cm^{-1}) reported for acetonitrile coordinated to $Al(H_2O)_5$ in solution (CD_3CN:$Al^{3+}{}_{5c}$).[64] The comparison of results for carbon monoxide adsorption, in particular with those relative to MIL-100(Cr), shows that the ν(CO) wavenumber for MIL-100(Al) is lower than expected respect to the Cr and Fe parent compounds. Such a behavior has been also reported in the case of SiO_2/B_2O_3 for which B^{3+} Lewis acid sites did not interact with CO whereas strong interaction was observed with pyridine.[46] This has been explained from a deformation of metallic sites, which occurs during the adsorption process. If the deformation site energy is stronger than the interaction energy between the probe and the site, no adsorption occurs. In the case of MOFs, another explanation can be put forward: the small diameter of the Al^{3+} cation would increase the shielding effect of the neighboring carboxyl oxygen atoms inducing a lower CUS Al^{3+} accessibility, as already mentioned by Bordiga et al. related to Cu^{2+} sites in HKUST-1.[34] On another hand, pyridine results are indirect, since we have been obliged to work on the ν_1 mode, which is not as sensitive as the ν_{8a} to the site acidity, therefore acetonitrile appears to be the best probe molecule to reveal the "right" strength of the Lewis acid sites, in such a case. We therefore conclude that the Lewis acidity of $Al^{3+}{}_{5c}$ in MIL-100 is quite high, being close to that reported for the stronger Lewis sites of silica−alumina (ν(CN) = 2330 cm^{-1})[65] and sulphated alumina samples (0.5 wt %) activated at 523 K (ν(CN) = 2328 cm^{-1}).[66]

CO and acetonitrile adsorptions reveal a low amount of stronger Lewis acid sites on dehydrated MIL-100(Al). They could correspond to structural defects as those created by the bond ruptures at the interface of crystallites inducing lower coordinated Al^{3+} sites. Their amount could be evaluated to 0.05 mmol g^{-1} from CO results, which corresponds to 1% of the total aluminum sites.

Water Species and Brønsted Acidity. Brønsted acidity arises from hydroxyl groups, either belonging to the framework (ν(Al−OH) band at 3588 cm^{-1}) or to water molecules. CO adsorption at low temperature on the dehydrated MIL-100(Al)

dx.doi.org/10.1021/jp210671t | J. Phys. Chem. C 2012, 116, 5710−5719

sample perturbs the free ν(Al−OH) band, which shifts to 3502 cm^{-1} ($\Delta\nu$(OH) = 86 cm^{-1}), whereas the ν(CO) band of the formed complex Al−OH···CO is at 2154 cm^{-1}. Such values are very close to those reported for the Cr−OH groups in MIL-100(Cr), showing that the Brønsted acid strength of framework OH sites, quite weak, does not depend on the nature of the metal, Al or Cr.

Water adsorption can give rise to different species: coordinated species (complex 1:1), water molecules H-bonded to coordinated species (complex 1:2), and multimer (scheme 1). Water molecules grafted on pentacoordinated Al^{3+} sites generate two kinds of Brønsted acid sites with different strengths. One distinguishing the sites resulting from the formation of complexes 1:1, characterized by a ν(CO) band at 2163 cm^{-1} (more acidic) and the other resulting from the formation of complexes 1:2 or multimeric species, characterized by a ν(CO) band at 2154 cm^{-1}. Single-crystal XRD analysis of hydrated MIL-100(Al) has allowed us to locate water molecules on the apertures of pentagonal and hexagonal windows (Figure 10). Two kinds of water species have to be considered

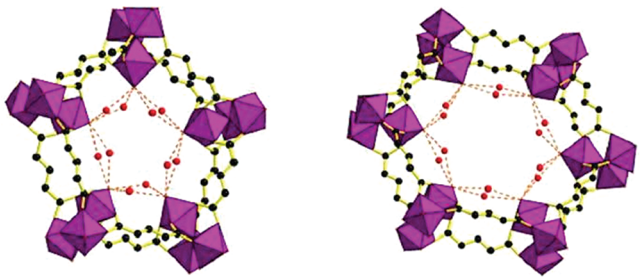

Figure 10. View of the interaction of water molecules, localized by DRX on monocrystal, with aluminum trimers.

Scheme 2. Molecules of Water Coordinated to CUS Al^{3+} (A Species) and Bridged to Hydrogen Atoms of Coordinated Water Molecules (B Species)

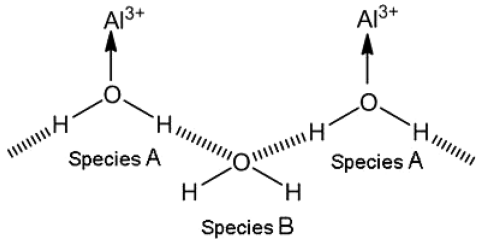

according to their coordination to CUS Al^{3+} (A species, see Scheme 2) or hydrogen bonded between two coordinated water molecules (B species). In the case of the fully hydrated sample, the Brønsted acidity arises only from species B. They can be considered as equivalent to water multimeric species. Their acidity, characterized by a ν(CO) band at 2154 cm^{-1} (Figure 9), is weak. Evacuation at higher temperature eliminates species B leading to free complexes 1:1 with higher acidity (ν(CO) band at 2164 cm^{-1}). The persistence of complex 1:1 (ν(OH) band at 3676 and 3582 cm^{-1}) at temperatures higher than 473 K shows a strong interaction of water molecules with CUS Al^{3+}. Their thermal stability is greater than that relative to complexes 1:1 in the case of MIL-100(Cr). This is in agreement with acetonitrile and pyridine adsorption experiments, which reveal a higher Lewis acid strength of CUS Al^{3+} relative to CUS Cr^{3+}.

CONCLUSION

Dehydrated MIL-100(Al) presents a large amount of coordinatively unsaturated Al^{3+}_{5c} sites acting as Lewis acid sites, even if inferior to the theoretical amount admitted for the investigated structure. Their acid strength has been determined by the adsorption of basic probe molecules (CO, pyridine, CD_3CN), and the results obtained show the interest to use several basic probe molecules: CD_3CN probe indicates a strong acidity of these sites, close to that reported for silica−alumina, whereas CO reveals a medium acid strength, as that reported for unsaturated sites in alumina. This contradictory result is particular to the MOFs material and cannot directly be extended to the metal oxides. Al^{3+} having the highest polarizing power among the trivalent cations, it cannot be expected to obtain a MIL-100 having a stronger acidity by changing the nature of the cation. Such an increase of the acidity could be obtained by the introduction of electron withdrawing groups either on the benzene ring, as it was done for a series of functionalized MIL-53(Fe),[67] or in the neighboring environment of the site (as shown on MIL-100(Cr), which contains fluorine in the synthesis medium).[33] An alternative approach could be to decrease the coordination number of the Lewis acid sites by the creation of defects, which may have a very strong acidity, as shown in the literature by CO and CD_3CN adsorption experiments.

The excellent agreement observed between results obtained from pyridine and CO adsorption and ^{27}Al NMR experiments validates the quantitative experimental results obtained by IR spectroscopy: the lower concentration of Lewis acid sites with respect to the parent compounds results from the presence of impurities, i.e., nitrates or acidic species coordinated on the Lewis acid sites or grafted on the structural OH groups.

The origin of the Brønsted acidity of MIL-100(Al) mainly results from water molecules located in the coordination sphere of the cation (complex 1:1 and 1:2). The acidity of the Al−OH group is weak and analogous to that of the structural hydroxyl groups of MIL-100(Cr). Its low concentration is due their reactivity toward impurities like free acid in the synthesis media.

ASSOCIATED CONTENT

Supporting Information

Additional IR data about the infrared bands of activated MIL-100(Al) and MIL-100(Cr) in the 1230−1050 cm^{-1} range (Figures S1 and S2) and in the ν(OH) region (Figure S3). This material is available free of charge via the Internet at http://pubs.acs.org.

AUTHOR INFORMATION

Corresponding Author

*E-mail: alexandre.vimont@ensicaen.fr.

Present Address

§Unité de Catalyse et Chimie du Solide, UMR CNRS 8181, Université Lille Nord de France, USTL − ENSCL, Bât. C7, BP 90108, Villeneuve d'Ascq, France.

Notes

The authors declare no competing financial interest.

ACKNOWLEDGMENTS

The French authors thank the CNRS and the ANR ("NoMAC" ANR-06-CO2-008) for their financial participation. Dr H. Leclerc thanks the Lower Normandy Region Council for the financial support.

REFERENCES

(1) Férey, G. *Chem. Soc. Rev.* **2008**, *37*, 191.
(2) Yaghi, O. M.; O'Keeffe, M.; Ockwig, M.; Chae, H. K.; Eddaoudi, M.; Kim, J. *Nature* **2003**, *423*, 705.
(3) Kitagawa, S.; Kitaura, R.; Noro, S. I. *Angew. Chem., Int. Ed.* **2004**, *43*, 2334.
(4) Corma, A.; Garcia, H.; Llabres i Xamena, F. X. *Chem. Rev.* **2010**, *110*, 4606.
(5) Loiseau, T.; Serre, C.; Huguenard, C.; Fink, G.; Taulelle, F.; Henry, M.; Bataille, T.; Ferey, G. *Chem.—Eur. J.* **2004**, *10*, 1373.
(6) Loiseau, T.; Mellot-Draznieks, C.; Muguerra, H.; Férey, G.; Haouas, M.; Taulelle, F. *C. R. Chimie* **2005**, *8*, 765.
(7) Comotti, A.; Bracco, S.; Sozzani, O.; Horike, S.; Matsuda, R.; Chen, J.; Takata, M.; Kubota, Y.; Kitagawa, S. *J. Am. Chem. Soc.* **2008**, *130*, 13664.
(8) Volkringer, C.; Loiseau, T.; Guillou, N.; Férey, G.; Haouas, M.; Taulelle, F.; Audebrand, N.; Margiolaki, I.; Popov, D.; Burghammer, M.; Riekel, C. *Cryst. Growth Des.* **2009**, *9*, 2927.
(9) Volkringer, C.; Loiseau, T.; Guillou, N.; Férey, G.; Elkaïm, E. *Solid State Sci.* **2009**, *11*, 1507.
(10) Senkovska, I.; Hoffmann, F.; Fröba, M.; Getzschmann, J.; Böhlmann, W.; Kaskel, S. *Microporous Mesoporous Mater.* **2009**, *122*, 93.
(11) Ahnfeldt, T.; Gunzelmann, D.; Loiseau, T.; Hirsemann, D.; Senker, J.; Férey, G.; Stock, N. *Inorg. Chem.* **2009**, *48*, 3057.
(12) Gascon, J.; Atkay, U.; Hernandez-Alonso, M. D.; Van Klink, G. P. M; Kapteijn, F. *J. Catal.* **2009**, 75.
(13) Volkringer, C.; Loiseau, T.; Devic, T.; Férey, G.; Popov, D.; Burghammer, M.; Riekel, C. *Cryst. Eng. Commun.* **2010**, *12*, 3225.
(14) Bloch, E. D.; Britt, D.; Lee, C.; Doonan, C. J.; Uribe-Romo, F. J.; Furukawa, H.; Long, J. R.; Yaghi, O. M. *J. Am. Chem. Soc.* **2010**, *132*, 14382.
(15) Liu, L.; Wang, X.; Jacobson, A. J. *Dalton Trans.* **2010**, *39*, 1722.
(16) Volkringer, C.; Loiseau, T.; Guillou, N.; Férey, G.; Haouas, M.; Taulelle, F.; Elkaïm, E.; Stock, N. *Inorg. Chem.* **2010**, *49*, 9852.
(17) Shigematsu, A.; Yamada, T.; Kitagawa, H. *J. Am. Chem. Soc.* **2011**, *133*, 2034.
(18) Volkringer, C.; Popov, D.; Loiseau, T.; Guillou, N.; Férey, G.; Haouas, M.; Taulelle, F.; Mellot-Draznieks, C.; Burghammer, M.; Riekel, C. *Nat. Mater.* **2007**, *6*, 760.
(19) Ahnfeldt, T.; Guillou, N.; Ginzelmann, D.; Margiolaki, I.; Loiseau, T.; Férey, G.; Senker, J.; Stock, N. *Angew. Chem., Int. Ed.* **2009**, *48*, 5163.
(20) Volkringer, C.; Popov, D.; Loiseau, T.; Férey, G.; Burghammer, M.; Riekel, C.; Haouas, M.; Taulelle, F. *Chem. Mater.* **2009**, *21*, 5695.
(21) Serra-Crespo, P.; Ramos-Fernandez, E. V.; Gascon, J.; Kapteijn, F. *Chem. Mater.* **2011**, *23*, 2565.
(22) Reinsch, H.; Krüger, M.; Wack, J.; Senker, J.; Salles, F.; Maurin, G.; Stock, N. *Microporous Mesoporous Mater.* **2012**, in press.
(23) Jan-Alcañiz, J.; Goesten, M.; Martinez-Joaristi, A.; Staviski, E.; Petukhov, A. V.; Gascon, J.; Kapteijn, F. *Chem. Commun.* **2011**, *47*, 8578.
(24) Staviski, E.; Goesten, M.; Juan-Alcañiz, J.; Martinez-Joaristi, A.; Serra-Crespo, P.; Petukhov, A. V.; Gascon, J.; Kapteijn, F. *Angew. Chem., Int. Ed.* **2011**, *50* (41), d9624.
(25) Haouas, M.; Volkringer, C.; Loiseau, T.; Férey, G.; Taulelle, F. *Chem.—Eur. J.* **2009**, *15*, 3139.
(26) Férey, G.; Mellot-Draznieks, C.; Serre, C.; Millange, F.; Dutour, J.; Surblé, S.; Margiolaki, I. *Science* **2005**, *309*, 2040.
(27) Serre, C.; Mellot-Draznieks, C.; Surblé, S.; Audebrand, N.; Filinchuk, Y.; Férey, G. *Science* **2007**, *315*, 1828.
(28) Hatop, H.; Ferbinteanu, M.; Roesky, H. W.; Cimpoesu, F.; Schiefer, M.; Schmidt, H. G.; Noltmeyer, M. *Inorg. Chem.* **2002**, *41*, 1022.
(29) Lemoine, P.; Berkaert, A.; Brion, J. D.; Viossat, B. *Z. Kristallogr. NCS* **2006**, *221*, 309.
(30) Loiseau, T.; Lecroq, L.; Volkringer, C.; Marrot, J.; Férey, G.; Haouas, M.; Taulelle, F.; Bourrelly, S.; Llewellyn, P. L.; Latroche, M. *J. Am. Chem. Soc.* **2006**, *128*, 10223.
(31) Leclerc, H.; Vimont, A.; Lavalley, J. C.; Daturi, M.; Wiersum, A. D.; Llwellyn, P. L.; Horcajada, P.; Ferey, G.; Serre, C. *Phys. Chem. Chem. Phys.* **2011**, *13*, 11748.
(32) Vimont, A.; Leclerc, H.; Mauge, F.; Daturi, M.; Lavalley, J. C.; Surble, S.; Serre, C.; Ferey, G. *J. Phys. Chem. C* **2007**, *111*, 383.
(33) Vimont, A.; Goupil, J. M.; Lavalley, J. C.; Daturi, M.; Surble, S.; Serre, C.; Millange, F.; Ferey, G.; Audebrand, N. *J. Am. Chem. Soc.* **2006**, *128*, 3218.
(34) Bordiga, S.; Regli, L.; Bonino, F.; Groppo, E.; Lamberti, C.; Xiao, B.; Wheatley, P. S.; Morris, R. E.; Zecchina, A. *Phys. Chem. Chem. Phys.* **2007**, *9*, 2676.
(35) Salles, F.; Maurin, G.; Serre, C.; Llewellyn, P. L.; Knoìfel, C.; Choi, H. J.; Filinchuk, Y.; Oliviero, L.; Vimont, A.; Long, J. R.; Férey, G. *J. Am. Chem. Soc.* **2010**, *132*, 13782.
(36) Vimont, A.; Thibault-Starzyk, F.; Daturi, M. *Chem. Soc. Rev.* **2010**, *39*, 4928.
(37) Lamberti, C.; Zecchina, A.; Groppo, E.; Bordiga, S. *Chem. Soc. Rev.* **2010**, *39*, 4951.
(38) Hadjiivanov, K. I.; Vayssilov, G. N. Characterization of oxide surfaces and zeolites by carbon monoxide as an IR probe molecule. In *Advances in Catalysis*; Academic Press Inc.: San Diego, 2002; *Vol. 47*; pp 307.
(39) Travert, A.; Vimont, A.; Sahibed-Dine, A.; Daturi, M.; Lavalley, J. C. *Appl. Catal. A: Gen.* **2006**, *307*, 98.
(40) Busca, G. *Phys. Chem. Chem. Phys.* **1999**, *1*, 723.
(41) Vimont, A.; Lavalley, J. C.; Sahibed-Dine, A.; Arean, C. O.; Delgado, M. R.; Daturi, M. *J. Phys. Chem. B* **2005**, *109*, 9656.
(42) Haneda, M.; Emmanuel Joubert, C.; Menezo, J.-C.; Duprez, D.; Barbier, J.; Bion, N.; Daturi, M.; Saussey, J.; Lavalley, J.-C.; Hamada, H. *Phys. Chem. Chem. Phys.* **2001**, *3*, 1366.
(43) Vimont, A.; Thibault-Starzyk, F.; Daturi, M. *Chem. Soc. Rev.* **2010**, *39*, 4928.
(44) Gribov, E. N.; Zavorotynska, O.; Agostini, G.; Vitillo, J. G.; Ricchiardi, G.; Spoto, G.; Zecchina, A. *Phys. Chem. Chem. Phys.* **2010**, *12*, 6474.
(45) Zecchina, A.; Escalona Platero, E.; Otero Arean, C. *J. Catal.* **1987**, *107*, 244.
(46) Travert, A.; Vimont, A.; Lavalley, J. C.; Montouillout, V.; Delgado, M. R.; Pascual, J. J. C.; Arean, C. O. *J. Phys. Chem. B* **2004**, *108*, 16499.
(47) Arnett, E. M.; Ludwig, R. T. *J. Am. Chem. Soc.* **1995**, *117*, 6627.
(48) Pearson, R. G. *J. Org. Chem.* **1989**, *54*, 1423.
(49) Dambournet, D.; Leclerc, H.; Vimont, A.; Lavalley, J. C.; Nickkho-Amiry, M.; Daturi, M.; Winfield, J. M. *Phys. Chem. Chem. Phys.* **2009**, *11*, 1369.
(50) Férey, G.; Serre, C.; Mellot-Draznieks, C.; Millange, F.; Surblé, S.; Dutour, J.; Margiolaki, I. *Angew. Chem., Int. Ed.* **2004**, *43*, 6296.
(51) Horcajada, P.; Surblé, S.; Serre, C.; Hong, D. Y.; Seo, Y. K.; Chang, J. S.; Greneéche, J. M.; Margiolaki, I.; Férey, G. *Chem. Commun.* **2007**, 2820.
(52) Schlenker, J. L.; Dwyer, F. G.; Jenkins, E. E.; Rohrbaugh, W. J.; Kokotailo, G. T. *Nature* **1981**, *294*, 340.
(53) Baerlocher, Ch.; McCusker, L. B.; Olson, D. H. *Atlas of Zeolite Framework Types*, 6th revised edition; Elsevier: Amsterdam, 2007.
(54) Haouas, M.; Volkringer, C.; Loiseau, T.; Férey, G.; Taulelle, F. *J. Phys. Chem. C* **2011**, *115*, 17934.
(55) Kim, Y.; Cho, K.; Lee, K.; Choo, J.; Gong, M.-s.; Joo, S.-W. *J. Mol. Struct.* **2008**, *878*, 155.
(56) Hadjiivanov, K. I. *Catal. Rev.* **2000**, *42*, 71.
(57) Mosqueda-Jimenez, B. I.; Lahougue, A.; Bazin, P.; Harle, V.; Blanchard, G.; Sassi, A.; Daturi, M. *Catal. Today* **2007**, *119*, 73.
(58) Gallas, J.-P.; Goupil, J.-M.; Vimont, A.; Lavalley, J.-C.; Gil, B.; Gilson, J.-P.; Miserque, O. *Langmuir* **2009**, *25*, 5825.
(59) Morterra, C.; Magnacca, G. *Catal. Today* **1996**, *27*, 497.
(60) Morterra, C.; Chiorino, A.; Ghiotti, G.; Garrone, E. *J. Chem. Soc., Faraday Trans. I* **1979**, *75*, 271.
(61) Morterra, C.; Coluccia, S.; Chiorino, A.; Boccuzzi, F. *J. Catal.* **1978**, *54*, 348.

(62) Chavan, S.; Vitillo, J. G.; Groppo, E.; Bonino, F.; Lamberti, C.; Dietzel, P. D. C.; Bordiga, S. *J. Phys. Chem. C* **2009**, *113*, 3292.
(63) Busca, G. *Catal. Today* **1996**, *27*, 321.
(64) Jamroz, D.; Wojcik, M.; Lindgren, J.; Stangret, J. *J. Phys. Chem. B* **1997**, *101*, 6758.
(65) Sempels, R. E.; Rouxhet, P. G. *J. Colloid Interface Sci.* **1976**, *55*, 263.
(66) Platero, E. E.; Mentruit, M. P.; Morterra, C. *Langmuir* **1999**, *15*, 5079.
(67) Devic, T.; Horcajada, P.; Serre, C.; Salles, F.; Maurin, G.; Moulin, B.; Heurtaux, D.; Clet, G.; Vimont, A.; Greneche, J. M.; Le Ouay, B.; Moreau, F.; Magnier, E.; Filinchuk, Y.; Marrot, J.; Lavalley, J. C.; Daturi, M.; Ferey, G. *J. Am. Chem. Soc.* **2010**, *132*, 1127.